Optics Communications 336 (2015) 127–133

Contents lists available at ScienceDirect

Optics Communications

journal homepage: www.elsevier.com/locate/optcom

Wave-front reconstruction with Hartmann–Shack sensor using a phase-retrieval method

Jing Li [a,b,*], Yan Gong [a], Hongfu Chen [a,b], Xinrong Hu [b]

[a] State Key Laboratory of Applied Optics, Changchun Institute of Optics, Fine Mechanics and Physics, Chinese Academy of Sciences, Changchun 130033, Jilin China

[b] University of Chinese Academy of Sciences, Beijing 100049, China

ARTICLE INFO

Article history:
Received 24 July 2014
Received in revised form
7 September 2014
Accepted 9 September 2014
Available online 11 October 2014

Keywords:
Testing
Active or adaptive optics
Phase retrieval
Wave-front sensing.

ABSTRACT

We apply a phase retrieval algorithm to the intensity patterns acquired from a Hartmann–Shack wave-front sensor to measure the wave-front aberration of a deep ultraviolet lithography system. The intensity patterns are obtained with and without the micro-lens array. Thus, we avoid selecting algorithm-specific parameters such as step-size and trust-region. Simulation results show that the phase-retrieval method enhances the accuracy of wave-front reconstruction compared with the conventional wave-front slope method. The relationships between the number of iterations of the phase retrieval algorithm, the calculating time and the wave-front reconstruction error are studied. This study demonstrates that the phase-retrieval method provides more accurate estimates of aberrations in near-flat wave-fronts relative to the wave-front slope method.

1. Introduction

The 20 nm node of semiconductor chips has been achieved by using 193 nm Deep Ultraviolet Lithography (DUVL) technology. In order to realize such high resolution, the performance of the projection objective in a DUVL system must reach the optical diffraction limit, thus the wave-front aberration for such a projection objective will typically approach to 0.01 wavelengths. Generally, in working condition the most appropriate apparatus to measure wave-front aberration of the lithography system is Hartmann–Shack wave-front sensor (HSWS). [1–4] However, a conventional HSWS cannot satisfy the accuracy requirement of wave-front aberration measurement for a DUVL projection objective. Many methods have been adopted to increase the accuracy of wave-front sensing. An effective way is altering the structure of HSWS, such as replacing the micro-lens array by several kinds of phase planes [3,5,6]. Other available way is obtaining more accurate positions of the spots on the Charge Coupled Device (CCD) sensor by optimizing the centroid calculation algorithm [7–10]. Another idea of enhancing the accurate of HSWS metrology is to modify the wave-front reconstruction algorithm [11–13]. However, the first method usually causes a loss of luminous energy since the phase plane obscures the light partially. The last two means are on the basis of the wave-front slope measurement method [14], which neglects the distribution inside each sub-aperture only using the centroid information of it and employs a geometrical approximation.

A phase-retrieval method is proposed to improve the wave-front estimate for the HSWS [15–17]. Wave-front phase is retrieved from the intensity measurement on the detector plane. The process utilizes the entire information inside the intensity distribution and lacks the geometrical approximation. This method improves the accuracy of the HSWS wave-front aberration measurement compared with the conventional wave-front slope method. A. Polo et al. presented a phase retrieval algorithm to determine the wave-front aberration using a Hartmann wave-front sensor (HWS) for an extreme ultraviolet lithography (EUVL) projection objective [16]. Li et al. used a modified HSWS for phase retrieval with a detector placed at a defocused plane of the micro-lens array [17]. They all obtained the intensity of the CCD sensor once and chose a minimizing function to retrieve the phase using different convergent algorithms. Algorithm-specific parameters were chosen in their algorithms [16,17]. However the accuracy of these convergent algorithms and speed of the convergences are limited mutually by these chosen parameters.

In this paper, we propose using a phase-retrieval method with a HSWS for DUVL system wave-front aberration measurement. The intensity patterns are obtained with and without the micro-lens array, respectively. By applying an iterative phase retrieval algorithm to the measured two intensity patterns, the phase of incoming wave-front is retrieved. This method does not require

* Corresponding author at: State Key Laboratory of Applied Optics, Changchun Institute of Optics, Fine Mechanics and Physics, Chinese Academy of Sciences, Changchun 130033, Jilin China.
E-mail address: lijing871215@126.com (J. Li).

http://dx.doi.org/10.1016/j.optcom.2014.09.086
0030-4018/

the operator to choose algorithm-specific parameters such as step-size and trust-region. Meanwhile the accuracy of the HSWS wave-front aberration measurement is improved compared with the wave-front slope measurement method. The theory of this method is presented in Section 2. In Section 3 we simulate phase retrieval procedures for several typical kinds of wave-front distributions in DUVL systems and a special wave-front aberration in a DUVL projection objective. Particularly the reconstruction results achieved by our phase-retrieval method are compared with that of the traditional wave-front slope method. The relationships between the number of iterations of phase retrieval algorithm, the calculating time and the wave-front reconstruction error are also studied. Finally, we draw conclusions in Section 4.

2. Principles of the HSWS

2.1. Conventional principle of the HSWS

The HSWS is evolved from the HWS by replacing the holes array with a micro-lens array [18], consequently the luminous energy is utilized more sufficiently. The HSWS is consisted of a micro-lens array focusing on a CCD sensor. The DUVL projection objective is a refractive optical system; therefore the HSWS with a micro-lens array is used.

Fig. 1 shows the principle of HSWSs. The HSWS measures the wave-front by dividing the incoming beam into sub-beams with a micro-lens array and analyzing the focal spots displacement. When testing a planar wave-front, the spots would be located at each centre of the sub-aperture corresponding to the micro-lens array on a CCD sensor as shown in Fig. 1(a). When a distorted wave-front is tested, the positions of the spots would shift from the centres of their apertures. Each division wave-front is considered as a tilt planar wave-front as shown in Fig. 1(b). Thus the slope of each sub-aperture wave-front along y direction could be calculated by the shift of the spot Δy and the focal length of the micro-lens array f (Fig. 1(c)).

$$\tan\theta_y = \frac{\Delta y}{f} = \frac{\Delta z}{d}, \tag{1}$$

where Δz is the Peak-to-Valley (PV) value of the division wave-front aberration along y direction, and d is the diameter of a single micro-lens. Similarly, the slope of each division wave-front along x direction could be calculated by $\tan\theta_x = \Delta x/f$.

The gradient of the tested wave-front phase approximates as

$$\nabla\Phi_{m,n} = \begin{pmatrix} \frac{\partial}{\partial x} \\ \frac{\partial}{\partial y} \end{pmatrix}\Phi_{m,n} \approx \begin{pmatrix} \tan\theta_x \\ \tan\theta_y \end{pmatrix}_{m,n}, \tag{2}$$

where Φ is the phase of the wave-front, (m, n) is the index of the micro-lens array along horizontal and vertical. The shifts of spots along x and y directions are commonly calculated by the centroid algorithm from the spots array obtained by the CCD sensor.

This reconstruction method using wave-front slope measurement has two shortcomings [16]. First, this method uses an approximation $\sin\theta \approx \tan\theta \approx \theta$. Thus the accuracy of the wave-front aberration measurement would be affected. Second, the distorted wave-front is considered as a combination of several planar wave-fronts. The details of the wave-front in each sub-aperture are missing. This would also affect the accuracy of the wave-front aberration measurement.

To overcome both shortcomings of the wave-front slope measurement, we apply a phase-retrieval method to the intensity information on the CCD sensor to acquire the wave-front aberration. Thus, we avoid the geometrical approximation; meanwhile we use the diffractive intensity data inside sub-apertures which contains more detailed wave-front information.

2.2. Phase-retrieval method with the HSWS

Phase-retrieval is a nonlinear algorithm to recover the phase distribution of an optical system from the intensity measurement on the detector plane [16]. The intensity distributions are recorded with and without the micro-lens array, respectively. The principle of the phase-retrieval method with the HSWS is shown in Fig. 2. The micro-lens array with a mount is inserted or pulled out of one groove, which is fabricated in front of the CCD sensor. The CCD sensor is placed on the focal plane of the micro-lens array. The directions of the arrows show the calculating directions of the propagation.

At first, the amplitude of the field distribution on the detector plane $A(x, y)$ without the micro-lens array is achieved by the measured intensity $|A(x, y)|^2$ on the CCD sensor. Set $U(x, y)$ to be the field distribution on the detector plane without the micro-lens array

$$U(x, y) = A(x, y)\exp[jk\Phi_0(x, y)], \tag{3}$$

where $j^2 = -1$, $k = 2\pi/\lambda$, λ is the wavelength, and $\Phi_0(x, y)$ is the phase distribution on the CCD sensor without the micro-lens array. Suppose the propagation is ideal. Using the theory of the inverse propagation of the angular spectrum, the field distribution of the plane before the micro-lens array $U_o(x_1, y_1)$ is written as [19]

$$\begin{aligned} U_o(x_1, y_1) &= F^{-1}\left\{F(U(x, y))\exp\left[-jkf\sqrt{1-(\lambda f_x)^2-(\lambda f_y)^2}\right]\right\} \\ &= C(x_1, y_1)\exp[jk\Phi(x_1, y_1)], \end{aligned} \tag{4}$$

where F denotes the Fourier transform, F^{-1} denotes the inverse Fourier transform, f_x and f_y are the spatial frequencies, $C(x_1, y_1)$ is the amplitude, and $\Phi(x_1, y_1)$ is its phase distribution. The transmittance function for an ideal, simple micro-lens in the micro-lens

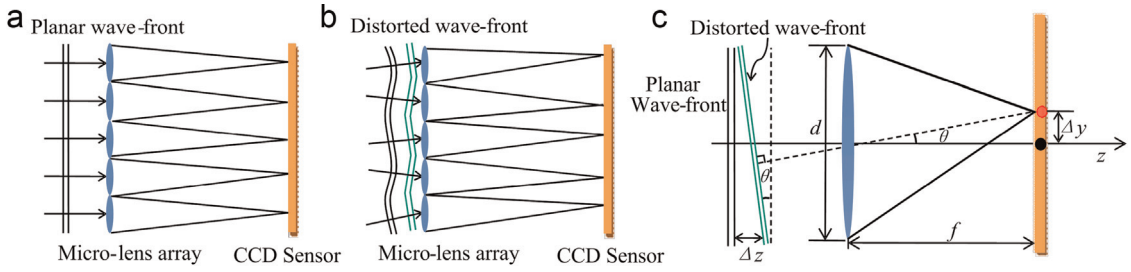

Fig. 1. Schematic of HSWSs. (a) Planar and (b) distorted wave-front; (c) single sub-aperture.

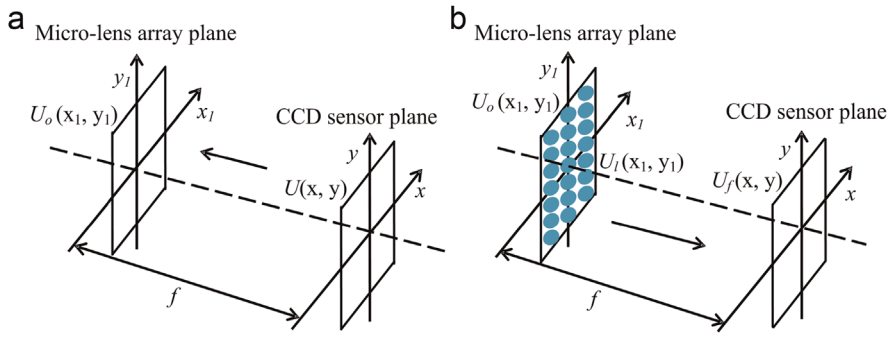

Fig. 2. Schematic of the phase-retrieval method with the HSWS. (a) Inverse propagation to obtain the field distribution of the plane before the micro-lens array from the intensity distribution of the CCD sensor plane (without micro-lens array), (b) forward propagation to obtain the field distribution of the CCD sensor plane from the calculated field distribution of the plane before the micro-lens array (considering with micro-lens array).

array is given by [19]

$$t_0(x_1, y_1) = rect\left(\frac{x_1}{d}, \frac{y_1}{d}\right)\exp\left[-j\frac{k}{2f}\left(x_1^2 + y_1^2\right)\right], \tag{5}$$

where d is the diameter of a single micro-lens, and f is known as the focal length. According to the array theorem [19] the transmittance function for the $N \times N$ micro-lens array $t(x_1, y_1)$ is written as

$$t(x_1, y_1) = t_0(x_1, y_1) \otimes \sum_{m,n=-N/2}^{N/2-1} \delta\left(x_1 - md, y_1 - nd\right), \tag{6}$$

where $\otimes$ donates convolution and N is even. Considering the tested wave-front as an object close to the micro-lens array, the field distributions of the plane behind the micro-lens array $U_l(x_1, y_1)$ is given by

$$U_l(x_1, y_1) = U_o(x_1, y_1)t(x_1, y_1). \tag{7}$$

Using the theory of the propagation of the angular spectrum, the field distributions of the detector plane with the micro-lens array $U_f(x, y)$ is expressed as

$$U_f(x, y) = F^{-1}\left\{F\left(U_l(x_1, y_1)\right)\exp\left[jkf\sqrt{1 - \left(\lambda f_{x_1}\right)^2 - \left(\lambda f_{y_1}\right)^2}\right]\right\}. \tag{8}$$

The phase-retrieval procedure is to recover the phase distribution $\Phi(x_1, y_1)$ from the measured intensity $|A(x, y)|^2$ on the detector plane without the micro-lens array and the measured intensity $|B(x, y)|^2$ on the detector plane with the micro-lens array. Iterative Fourier Transform Algorithm (IFTA) [20,21] is first proposed by Gechberg and Saxton to solve the phase retrieval problem. In our condition, IFTA is used as follow (Fig. 3):

(a) Assume the phase distribution $\Phi_0(x, y)$ as an ideal planar wave-front initially. According to Eq. (3) (4), we get the original object field distribution $U_{o(i)}(x_1, y_1) = C(x_1, y_1)\exp[jk\Phi(x_1, y_1)]$. The subscript i is the iteration time.

(b) Applying Eqs. (5)–(8), we obtain the field distribution on the detector plane $U_{f(i)}(x, y)$.

(c) The amplitude of $U_{f(i)}(x, y)$ is replaced with $B(x, y)$, while the phase distribution stay still:

$$U'_{f(i)}(x, y) = B(x, y)\frac{U_{f(i)}(x, y)}{\left|U_{f(i)}(x, y)\right|}. \tag{9}$$

(d) Then use the inverse propagation of the angular spectrum. Treat $U'_{f(i)}(x, y)$ as the objective field distribution. The field distributions of the plane behind the micro-lens array $U'_{l(i)}(x_1, y_1)$ is given by

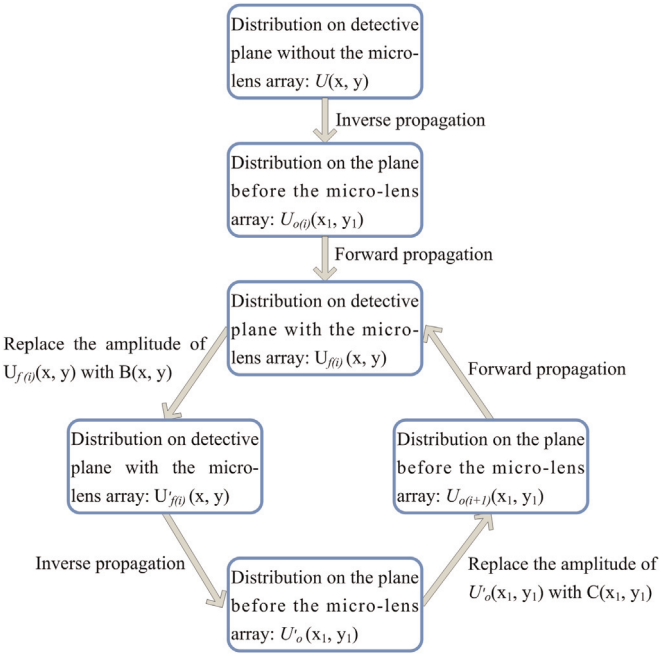

Fig. 3. Flowchart for the phase-retrieval with the HSWS obtaining the intensity distributions with and without the micro-lens array respectively.

$$U'_{l(i)}(x_1, y_1) = F^{-1}\left\{F\left[U'_{f(i)}(x, y)\right]\exp\left[-jkf\sqrt{1 - \left(\lambda f_x\right)^2 - \left(\lambda f_y\right)^2}\right]\right\}. \tag{10}$$

During this process, the transmittance function for the micro-lens array $t'(x_1, y_1)$ becomes:

$$t'\left(x_1, y_1\right) = \left\{rect\left(\frac{x_1}{d}, \frac{y_1}{d}\right)\exp\left[j\frac{k}{2f}\left(x_1^2 + y_1^2\right)\right]\right\} \otimes \sum_{m,n=-N/2}^{N/2-1} \delta\left(x_1 - md, y_1 - nd\right). \tag{11}$$

The field distribution in the objective plane $U'_{o(i)}(x_1, y_1)$ is given by

$$U'_{o(i)}(x_1, y_1) = U'_{l(i)}(x_1, y_1)t'(x_1, y_1). \tag{12}$$

(e) The amplitude of $U'_{o(i)}(x_1, y_1)$ is replaced with $C(x_1, y_1)$, while the phase distribution stay still. The result is treated as the

start of next iteration

$$U_{o(i+1)}(x_1, y_1) = C(x_1, y_1)\frac{U'_{o(i)}(x_1, y_1)}{\left|U'_{o(i)}(x_1, y_1)\right|}. \tag{13}$$

Proceed step (b)–(e) repeatedly. Define the error function as

$$\delta_o = \frac{\iint\left(\left|U_o(x_1, y_1)\right| - C(x_1, y_1)\right)^2 dx_1 dy_1}{\iint C^2(x_1, y_1)dx_1 dy_1}, \delta_d = \frac{\iint\left(\left|U_f(x, y)\right| - B(x, y)\right)^2 dxdy}{\iint B^2(x, y)dxdy}. \tag{14}$$

With the increasing of the number of iterations, δ_o and δ_d decrease. When the variation value of δ_o and δ_d is quite small, the iteration should be stopped. The ultimate phase distribution $\Phi(x_1, y_1)$ is retrieved. We finally write the phase as a linear combination of Zernike polynomials

$$\Phi(x_1, y_1) = \sum_{p=1}^{N} a_p Z_p(x_1, y_1), \tag{15}$$

where $Z_p(x_1, y_1)$ is the pth Zernike polynomial, and the coefficients a_p are the optimizing variables of the problem. IFTA converges quickly in first few times. However in the next times the speed of convergence slows down greatly. Therefore, researchers come up with many improved IFTA by introducing some parameter controls [22–24]. In this paper, we would not describe more details about them. One of the improved IFTAs, Adaptive-Additive (AA) algorithm [25] is chosen to solve our problem because of its quick convergence. The Eq. (9) in step (c) transforms to

$$U'_{f(i)}(x, y) = \left[\xi B(x, y) + (1 - \xi)\left|U_{f(i)}(x, y)\right|\right]\frac{U_{f(i)}(x, y)}{\left|U_{f(i)}(x, y)\right|}, \tag{16}$$

where ζ is a constant ($0 \le \zeta \le 2$).

3. Simulation results and discussions

In a DUVL system, the most common wave-front aberration is defocus, astigmatism, and coma [3]. Therefore we simulate wave-fronts representing defocus, astigmatism, and coma respectively. However, wave-front aberrations contain not only one term of Zernike polynomials in reality. To simulate a more real situation, we add in other Zernike polynomials. The coefficients of these additional Zernike polynomials are relatively small and chosen arbitrarily. Fig. 4 (a–e) shows the wave-front distributions mentioned above. The Root-Mean-Squares (RMS) values of the wave-fronts are set to near 0.025λwhich is referred to the "GOLD" level of RMS value of the DUVL projection objective wave-front aberration [26]. The defocus distribution has a prominent 4th term of the Fringe Zernike coefficients which signifies defocus (Fig. 4 (b)). The astigmatism and coma distributions have a prominent 5th and 7th term of the Fringe Zernike coefficients respectively (Fig. 4 (d and f)).

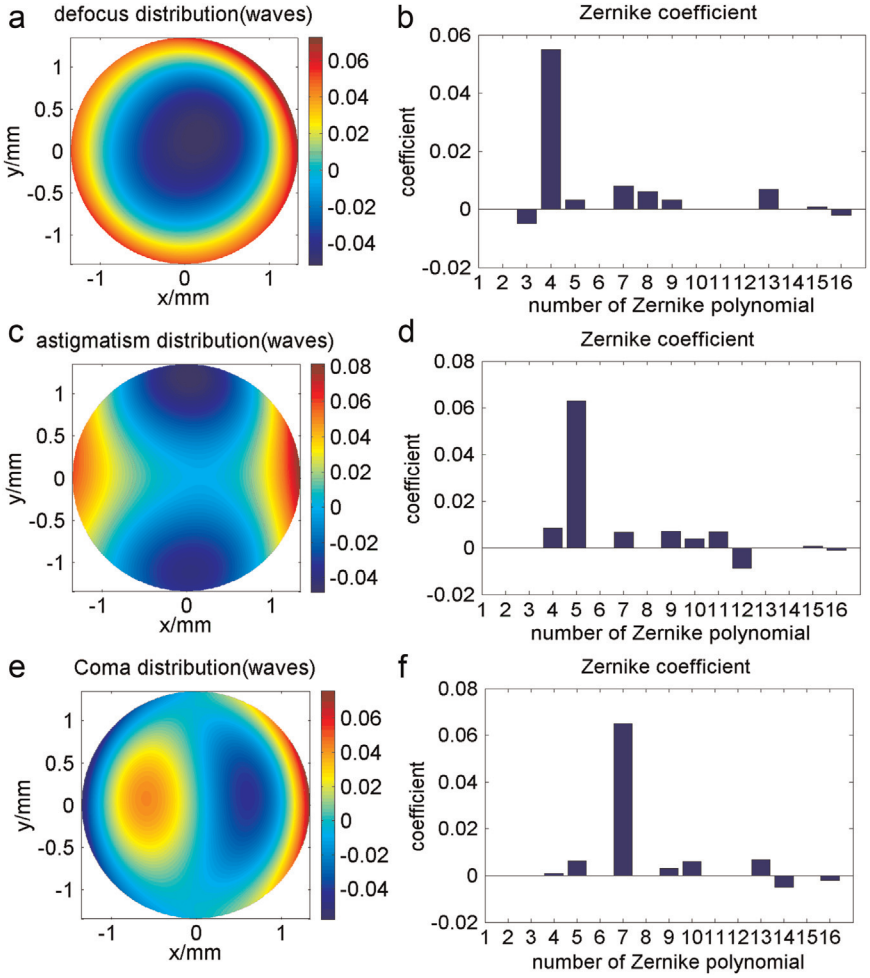

Fig. 4. Distributions of (a) defocus (PV=0.0724λ, RMS=0.0285λ), (c) astigmatism (PV=0.0812λ, RMS=0.0237λ), and (e) coma (PV=0.0758λ, RMS=0.0208λ); Zernike coefficients distribution of (b) the defocus, (d) astigmatism, (f) and coma.

Table 1
Results of wave-front reconstruction of typical kinds of wave-front aberration

Wave-front type	PV(λ)			RMS(λ)			Error PV(λ)		Error RMS(λ)	
	tested	slope	Phase-retrieval	tested	slope	Phase-retrieval	slope	Phase-retrieval	slope	Phase-retrieval
defocus	0.0724	0.0569	0.0673	0.0285	0.0246	0.0268	0.0179	0.0091	0.0045	0.0025
astigmatism	0.0812	0.0702	0.0811	0.0237	0.0220	0.0233	0.0115	0.0025	0.0030	0.0011
coma	0.0758	0.0464	0.0757	0.0208	0.0199	0.0196	0.0351	0.0052	0.0109	0.0024

Using the simulated intensity data, we compare the phase reconstructions obtained with the phase-retrieval method and the wave-front slope method. The results are shown in Table 1. The RMS value of the wave-front slope method [27] reconstruction error for the defocus, astigmatism and coma wave-front distribution are 0.0045λ, 0.0030λ, and 0.0109λ, respectively. For coma distribution the accuracy of phase reconstruction by wave-front slope method is worse than other two kinds of wave-front distributions. When the phase varies sharply, the approximation: $\sin(\theta) \approx \tan(\theta) \approx \theta$ using in the wave-front slope method cannot guarantee the accuracy of the wave-front reconstruction any more.

The number of iterations of the phase-retrieval method is set to be 100. The RMS values of the phase-retrieval reconstruction error for the defocus, astigmatism and coma wave-front distribution are 0.0025λ, 0.0011λ, and 0.0024λ respectively. All kinds of wave-front distributions are recovered with a high accuracy. The structures of these reconstruction errors are all similar to those of original wave-front distributions. The probable reason is the accuracy of iterative algorithm for the phase-retrieval method. Optimizing the algorithm or increasing the number of iterations may decrease the phase-retrieval method reconstruction error.

The results show that the accuracy of wave-front reconstruction with the phase-retrieval method is higher than with the wave-front slope method for the typical wave-front aberration reconstruction in the DULV system. With the phase-retrieval method, the diffractive information inside each sub-aperture is no longer ignored. And the geometrical approximation is successfully avoided. Thus the accuracy of the wave-front reconstruction is improved.

We simulate reconstructing an experimental tested wave-front. The simulations are consistent with the experimental setup we will use. The focal length of the micro-lens array in the HSWS is 14 mm. The micro-lens array has 36×36 micro-lens. The diameter of each micro-lens aperture is 220 μm. The tested lens is a DUVL projection objective. The working wavelength is 193 nm. The wave-front aberration in its designed marginal field $(0.00, -0.19)$ deg is chosen to be tested. The 36 Zernike coefficients of the tested wave-front are calculated by the optical design software. The tested wave-front has tilt, defocus since the 3rd and 4th Zernike coefficients are prominent. The 5th, 11th and 12th Zernike coefficients indicate that the tested wave-front has serious astigmatism. At the mean time the 8th and 15th Zernike coefficients reveal that the tested wave-front has coma. The RMS value of the tested wave-front is 0.0068λ.

Assuming the collimator is ideal, thus the intensity distribution on the CCD sensor is obtained by ray tracing. The images obtained by the CCD sensor with and without the micro-lens array are shown as Fig. 5(a and b) respectively. With the micro-lens array, the image is a spots array. Without the micro-lens array, the CCD camera is homogenously illuminated. The tested wave-front is shown in Fig. 6(a). The results of the wave-front slope method and the phase-retrieval method are shown in Fig.6 (b)∼(e). The RMS value of the reconstructed wave-front with first method is 0.0052λ, while the RMS value of its reconstruction error is 0.0020λ. The number of iterations of the phase-retrieval method is first set to be 200. The RMS value of the reconstructed wave-front with this method is 0.0063λ, while the RMS values of its reconstruction error is $8.0523 \times 10^{-4}\lambda$. The wave-front reconstruction with the phase-retrieval method is more approximate to the tested wave-front than with the wave-front slope method. The experimental simulation results agreed to the typical wave-front aberrations simulation results.

Write the recovered wave-front aberration into a linear combination of 36 Zernike polynomials. Since the high order coefficients are quite small, we only show the first 16 Zernike coefficients. The original Zernike coefficients of the tested wave-front, reconstructed Zernike coefficients obtained by the wave-front slope method and phase-retrieval method are shown in Fig. 7. Prominent Zernike coefficients achieved through the phase-retrieval method are more close to the known ones compared with the wave-front slope method. The results show that the wave-front slope method is not available to get an accurate reconstruction. The Zernike coefficients achieved by the phase-retrieval method is more corresponding to those of the tested wave-front.

We choose several numbers of iterations between 25 and 200. With the increase of the number of iterations, the calculating time spent is increasing linearly. The relationships between the number of iterations of phase-retrieval algorithm and PV, RMS values of

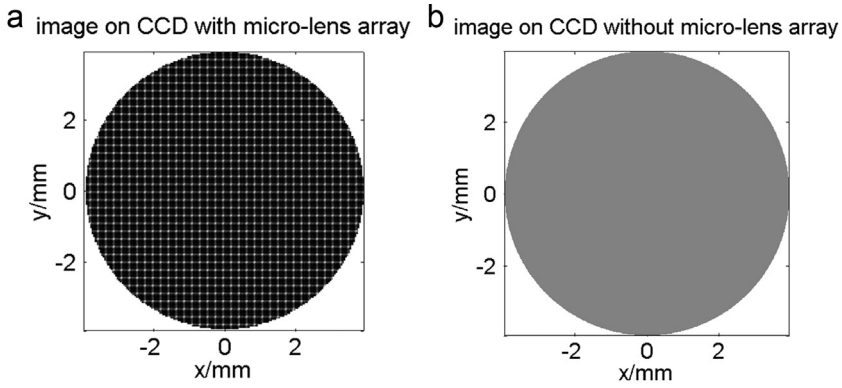

Fig. 5. Simulated image on CCD sensor (a) when the micro-lens array is in place, and (b) when the micro-lens array is removed.

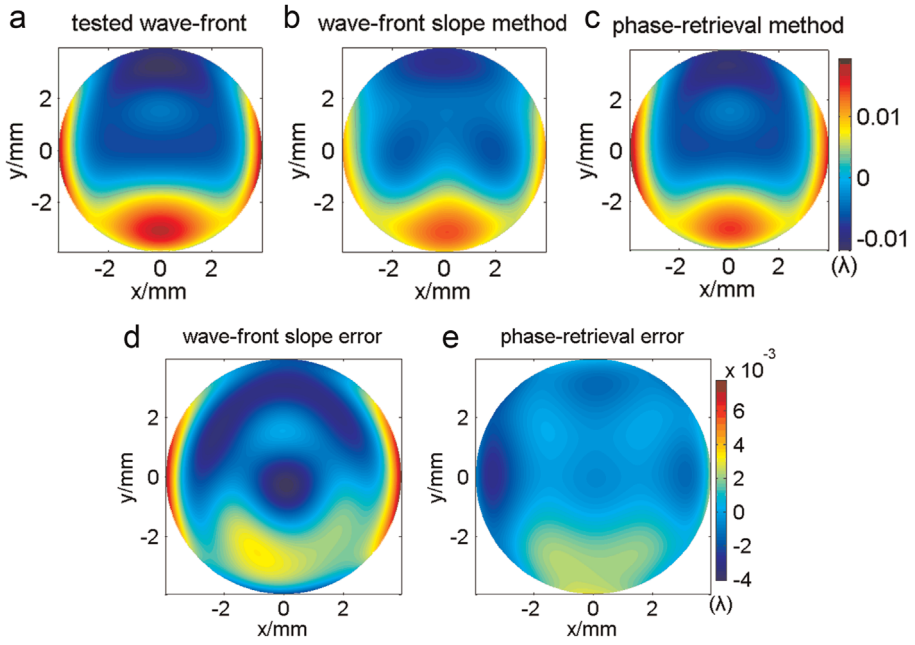

Fig. 6. (a) Tested wave-front with PV=0.0195λ and RMS=0.0068λ; Reconstruction for the tested wave-front distribution of (b) the wave-front slope method (PV=0.0141λ, RMS=0.0052λ), (c) the phase retrieval method (PV=0.0192λ, RMS=0.0063λ); reconstruction error for the tested wave-front distribution of (d) the wave-front slope method (PV=0.0078λ, RMS=0.0020λ), (e) the phase-retrieval method (PV=0.0026λ, RMS=$8.0523\times10^{-4}\lambda$).

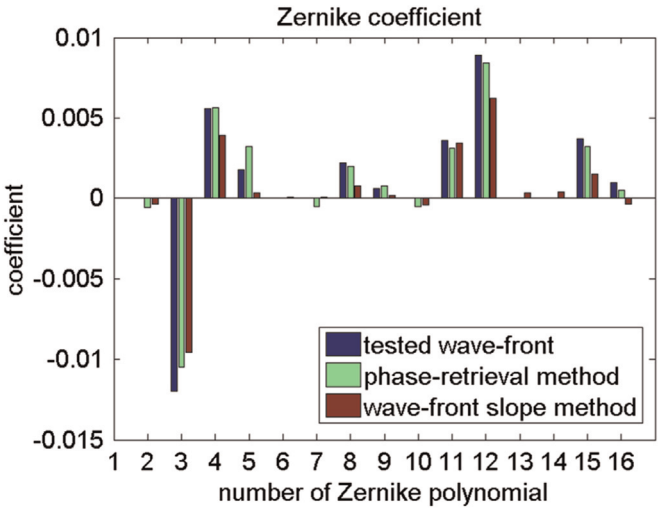

Fig. 7. First 16 Zernike coefficients of the tested and reconstructed wave-fronts.

that phase-retrieval method is suitable for the application. The decrease of the reconstruction error is slower with the increase of the number of iterations. When the number of iterations rises over 100, the decrease of reconstruction error is no longer distinct and the RMS value of reconstruction error drops to 1/1000λ. This reconstruction error is sufficient to the wave-front aberration measurement for a DUVL projection objective.

4. Conclusion

We have testified the feasibility of adopting a phase-retrieval method to an HSWS to measure the wave-front aberration in a DUVL system with an accuracy of over 1/1000λ. The principle and limits of the conventional wave-front slope method reconstruction by the usual centroid algorithm have been shown. Simulations for several typical kinds of wave-front aberrations of the DUVL system were conducted to compare the wave-front slope method reconstruction with the phase-retrieval method reconstruction.

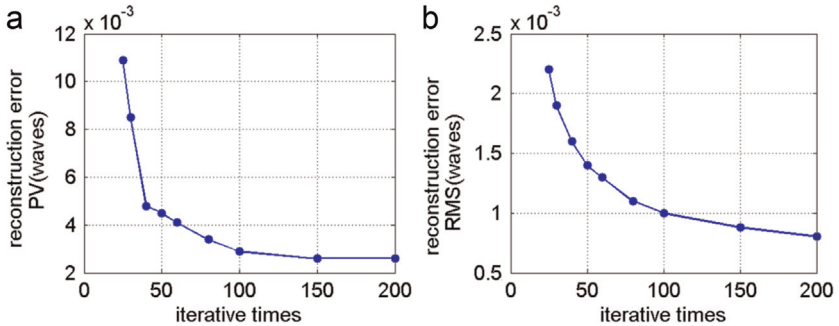

Fig. 8. The relationship between (a) number of iterations of phase retrieval algorithm and the PV value of wave-front reconstruction error, (b) number of iterations of phase retrieval algorithm and the RMS value of wave-front reconstruction error

the wave-front reconstruction error are shown in Fig. 8 (a and b) respectively. The calculation is conducted on a personal computer. The longest calculating time is about 5 minutes. The result shows Simulation results show that the wave-front slope reconstruction suffers from the geometrical approximation. The RMS value of the wave-front reconstruction error decreases based on the

phase-retrieval method compared with the wave-front slope method. A simulation with the parameters corresponding to the experimental setup has been conducted to demonstrate the phase-retrieval method. The result shows a reasonable agreement with the typical wave-front aberrations simulation. A study of the relationships between the number of iterations of phase retrieval algorithm, the calculating time and the PV and RMS value of the wave-front reconstruction error has been done. The calculating time of the phase retrieval algorithm is acceptable. When the number of iterations rises over 100, the decrease of reconstruction error is no longer distinct and the RMS value of the wave-front reconstruction error drops to $1/1000\lambda$.

The results of this research show that the HSWS could be applied to measure the wave-front aberration in a DUVL system through a phase-retrieval method with the accuracy of $1/1000\lambda$. Meanwhile this method may be used to drive an adaptive optics system to compensate the intrinsic wave-front aberration in the optical system or direct the process of a system adjustment.

Acknowledgments

This work is supported by the Youth Innovation Foundation under Grant no. 41104122 and the Chinese-Belarus cooperation project from Ministry of Science and Technology of the People's Republic of China no. 2011DFR10010.

References

[1] J. Lee, H. Yang, J. Hahn, Appl. Opt. 46 (2007) 1411.
[2] M. Augustin, S. Müller-Pfeiffer, L. Körner, O. Falkenstörfer, Proc. SPIE 7102 (2008) 71020P.
[3] Y. Ohsaki, Measurement apparatus, Exposure apparatus, and device manufacturing method, US Patent 7,956,987 B2.
[4] J. Primot, Opt. Commun. 222 (2003) 81.
[5] L. Zhao, W. Guo, X. Li, M. Chen, Opt. Lett. 36 (2011) 2752.
[6] S. Mousset, C. Rouyer, G. Marre, N. Blanchot, S. Montant, B. Wattellier, Opt. Lett. 31 (2006) 2634.
[7] P.M. Prieto, F. Vargas-Martín, S. Goelz, P. Artal, J. Opt. Soc. Am. A 17 (2000) 1388.
[8] S. Baik, S. Park, C. Kim, B. Cha, Opt. Laser Technol. 39 (2007) 262.
[9] J. Vargas, L. González-Fernandez, J.A. Quiroga, T. Belenguer, Appl. Opt. 49 (2010) 2409.
[10] W. Guo, L. Zhao, C. Tong, C. I-Ming, S.C. Joshi, Appl. Opt. 52 (2013) D75.
[11] R.G. Lane, M. Tallon, Appl. Opt. 31 (1992) 6902.
[12] L. Seifert, H.J. Tiziani, W. Osten, Opt. Commun. 245 (2005) 255.
[13] A. Talmi, E.N. Ribak, J. Opt. Soc. Am. A 23 (2006) 288.
[14] W.H. Southwell, J. Opt. Soc. Am. 70 (1980) 998.
[15] R.M. Clare, R.G. Lane, Appl. Opt. 43 (2004) 4080.
[16] A. Polo, V. Kutchoukov, F. Bociort, S.F. Pereira, H.P. Urbach, Opt. Express 20 (2012) 7822.
[17] C. Li, B. Li, S. Zhang, Appl. Opt. 53 (2014) 618.
[18] B.C. Platt, R. Shack, J. Refract. Surg. 17 (2001) S573.
[19] J.W. Goodman, Introduction to Fourier optics, Roberts and Company Publishers, 2005.
[20] R.W. Gechberg, W.O. Saxton, Optik 34 (1971) 275.
[21] R.W. Gechberg, W.O. Saxton, Optik 35 (1972) 237.
[22] R.J. Fienup, Proc. SPIE, 373, 147.
[23] J.R. Fienup, Appl. Opt. 21 (1982) 2758.
[24] L. Bigué, P. Ambs, Appl. Opt. 40 (2001) 5886.
[25] V. Soifer, V. Kotlyar, L. Doskolovich, Iterative Methods for Diffractive Optical Elements Computation, Taylor and Francis, London, 1997.
[26] C. Progler, D. Wheeler, Proc. SPIE 3334 (1998) 256.
[27] J. Li, Y. Gong, X. Hu, C. Li, Chin. J. Lasers 41 (2014) 0316002.